THE JOURNAL OF BIOLOGICAL CHEMISTRY VOL. 286, NO. 52, pp. 44367–44379, December 30, 2011

Two Proteases, Trypsin Domain-containing 1 (Tysnd1) and Peroxisomal Lon Protease (PsLon), Cooperatively Regulate Fatty Acid β-Oxidation in Peroxisomal Matrix*[S]

Received for publication, July 23, 2011, and in revised form, October 4, 2011 Published, JBC Papers in Press, October 14, 2011, DOI 10.1074/jbc.M111.285197

Kanji Okumoto[‡§], **Yukari Kametani**[§], **and Yukio Fujiki**[‡§¶1]

From the [‡]*Department of Biology, Faculty of Sciences, and* [§]*Graduate School of Systems Life Sciences, Kyushu University Graduate School, 6-10-1 Hakozaki, Higashi-ku, Fukuoka 812-8581, Japan and the* [¶]*Japan Science and Technology Agency (JST), Core Research for Evolutional Science and Technology (CREST), Chiyoda, Tokyo 102-0075, Japan*

Background: Tysnd1 and PsLon are newly identified peroxisomal matrix serine proteases.
Results: Tysnd1 inactivates its protease activity by self-conversion of the 60-kDa form to 15- and 45-kDa chains that are then degraded by PsLon. Tysnd1 regulates the peroxisomal fatty acid β-oxidation pathway via proteolytic processing of β-oxidation enzymes.
Conclusion: Tysnd1 and PsLon cooperatively regulate fatty acid β-oxidation in peroxisomal matrix.
Significance: The data shed light on how enzyme turnover is regulated inside peroxisomes.

The molecular mechanisms underlying protein turnover and enzyme regulation in the peroxisomal matrix remain largely unknown. Trypsin domain-containing 1 (Tysnd1) and peroxisomal Lon protease (PsLon) are newly identified peroxisomal matrix proteins that harbor both a serine protease-like domain and a peroxisome-targeting signal 1 (PTS1) sequence. Tysnd1 processes several PTS1-containing proteins and cleaves N-terminal presequences from PTS2-containing protein precursors. Here we report that knockdown of Tysnd1, but not PsLon, resulted in accumulation of endogenous β-oxidation enzymes in their premature form. The protease activity of Tysnd1 was inactivated by intermolecular self-conversion of the 60-kDa form to 15- and 45-kDa chains, which were preferentially degraded by PsLon. Peroxisomal β-oxidation of a very long fatty acid was significantly decreased by knockdown of Tysnd1 and partially lowered by PsLon knockdown. Taken together, these data suggest that Tysnd1 is a key regulator of the peroxisomal β-oxidation pathway via proteolytic processing of β-oxidation enzymes. The proteolytic activity of oligomeric Tysnd1 is in turn controlled by self-cleavage of Tysnd1 and degradation of Tysnd1 cleavage products by PsLon.

The peroxisome is an organelle that plays pivotal roles in various essential metabolic pathways such as β-oxidation of very long fatty acids and synthesis of plasmalogens (1, 2). Peroxisomal matrix and membrane proteins are synthesized on cytoplasmic free polyribosomes and imported post-translationally into peroxisomes (3). For peroxisome matrix proteins, two types of topogenic peroxisome-targeting signals (PTSs)[2] have been defined. PTS1 is a C-terminal tripeptide of the sequence SKL. This sequence and its derivatives are found in most matrix proteins (4, 5). PTS2 is an N-terminal cleavable presequence consisting of the nonapeptide sequence (R/K)(L/V/I)X_5(H/Q)(L/A) and has been identified in several proteins (6, 7). Extensive studies over the past two decades have revealed that more than 14 *PEX* genes and their products, peroxins, are required for peroxisome biogenesis in mammals (for reviews, see Refs. 8 and 9). Of these, Pex5p and Pex7p function as cytosolic receptors for PTS1 and PTS2, respectively (10–13). In mammals, two isoforms of Pex5p, Pex5pS and Pex5pL, which contains a 37-aa insertion, have been identified (14, 15). Both Pex5p isoforms are essential for PTS1 protein import and function by binding to PTS1 sequences. Pex5pL is also required for PTS2 protein import, forming higher order complexes with Pex7p-PTS2 complexes (16, 17).

Fatty acid β-oxidation is one of the essential functions of peroxisomes in organisms from yeast to higher eukaryotes, including humans (8, 18). In mammals, although both peroxisomes and mitochondria are responsible for fatty acid β-oxidation, peroxisomal β-oxidation is essential for chain shortening of very long fatty acids ($>C_{22}$) as evidenced by the loss of this function in individuals with peroxisome biogenesis disorders (8, 18). Peroxisomal β-oxidation enzymes are peroxisome matrix proteins that harbor PTS1 or PTS2 sequences. Three

* This work was supported in part by a CREST grant (to Y. F.) from the Science and Technology Agency of Japan; by grants-in-aid for scientific research (to Y. F.) and The Global Center of Excellence Program from The Ministry of Education, Culture, Sports, Science, and Technology of Japan; and a grant (to Y. F.) from the Japan Foundation for Applied Enzymology.
[S] The on-line version of this article (available at http://www.jbc.org) contains supplemental Fig. S1 and Tables S1–S3.
[1] To whom correspondence should be addressed: Dept. of Biology, Faculty of Sciences, Kyushu University Graduate School, 6-10-1 Hakozaki, Higashi-ku, Fukuoka 812-8581, Japan. Tel.: 81-92-642-2635; Fax: 81-92-642-4214; E-mail: yfujiki@kyudai.jp.

[2] The abbreviations used are: PTS, peroxisomal-targeting signal; aa, amino acid(s); AOx, acyl-CoA oxidase; DBP, D-bifunctional protein; Deg15, *A. thaliana* Deg protease 15; FL, FLAG epitope tag; HtrA, high temperature requirement A protease; mLon, mitochondrial Lon protease; PsLon, peroxisomal Lon protease; SCPx, sterol carrier protein x; TH, 3-ketoacyl-CoA thiolase; Tysnd1, trypsin domain-containing 1; Tysnd1-N and -C, N-terminal 10-kDa and C-terminal 45-kDa fragments of Tysnd1, respectively; Tysnd1-SA and -ΔCv, Tysnd1 variants with a Ser^{481}-to-Ala (SA) substitution and a deletion of 8 amino acid residues encompassing the self-cleavage site between Cys^{110} and Ala^{111}, respectively; Bis-Tris, 2-[bis(2-hydroxyethyl)amino]-2-(hydroxymethyl)propane-1,3-diol; EGFP, enhanced green fluorescent protein.

β-oxidation PTS1 enzymes, acyl-CoA oxidase (AOx) and D-bifunctional protein (DBP)/multifunctional enzyme 2/Hsd17b4 (hereafter termed DBP), which catalyze the oxidation of fatty acyl-CoA and the subsequent sequential hydration and dehydrogenation reactions, respectively (19, 20), and sterol carrier protein x (SCPx), which catalyzes the last acetyl-CoA-cleaving step, were recently suggested to undergo proteolytic processing by the peroxisomal PTS1-type protease trypsin domain-containing 1 (Tysnd1) (21). Tysnd1 also cleaves the PTS2 presequence from peroxisomal 3-ketoacyl-CoA thiolase (TH), which catalyzes the last step of peroxisomal β-oxidation (21). Another PTS1-type protease in the peroxisomal matrix, peroxisomal Lon protease (PsLon) of the ATP-dependent Lon protease family (22), has also been identified in rat liver peroxisomes (23). However, the substrates of PsLon have yet to be defined.

Little is known about the mechanisms underlying homeostasis of peroxisome physiology such as protein turnover and enzyme regulation. In the present work, as a step to gaining insight into such issues, we attempted to address whether Tysnd1 and PsLon are physiologically and mutually relevant in peroxisome physiology, including peroxisomal fatty acid β-oxidation. Self-cleavage of Tysnd1 negatively regulated the proteolytic activity of Tysnd1 against matrix PTS1 and PTS2 proteins. Knockdown of Tysnd1 resulted in a significant decrease in the processing of several β-oxidation enzymes and the β-oxidation of very long fatty acids. Moreover, PsLon was able to bind to Tysnd1 and preferentially degraded the self-processed forms of Tysnd1. These results support a potential mechanism by which Tysnd1 and PsLon together regulate peroxisomal fatty acid β-oxidation.

EXPERIMENTAL PROCEDURES

Cell Culture and DNA Transfection—HeLa and HEK293 cells were maintained in DMEM (Invitrogen), and CHO-K1 cells were maintained in Ham's F-12 (Invitrogen); both media were supplemented with 10% FCS under conditions of 5% CO_2, 95% air (24). DNA transfection of CHO-K1 and HEK293 cells was done with Lipofectamine (Invitrogen), and that of HeLa cells was done with Lipofectamine 2000 (Invitrogen) according to the manufacturer's protocols. HEK293 cells stably expressing His- and FLAG-tagged *Cl*Pex5pL, termed HEK/HF-5L, were isolated by transfection of pcDNAZeo/*His-FLAG-ClPEX5L* followed by selection with Zeocin (Invitrogen) as described previously (24). Stable transformants of HEK293 cells expressing wild-type Tysnd1 (FLAG-*Hs*Tysnd1) or an S481A mutant of FLAG-*Hs*Tysnd1 (FLAG-Tysnd1-SA) were likewise isolated by transfection of pcDNAZeo/*FLAG-HsTysnd1-WT* and pcDNAZeo/*FLAG-HsTysnd1-S481A*, respectively.

Antibodies—Where indicated, rabbit antisera to AOx (25), SCPx (26), TH (25), alkyldihydroxyacetonephosphate synthase (27), catalase (25), Pex5p (28), Pex13p (17), and Pex14p (29) were used. Mouse monoclonal antibodies to the FLAG epitope (M2; Sigma) and influenza virus hemagglutinin (HA) (16B12; Covance) and goat antiserum to lactate dehydrogenase (Rockland, Gilbertsville, PA) were purchased. Polyclonal antisera to Tysnd1 and PsLon were raised by conventional subcutaneous injection of recombinant human Tysnd1 (aa residues 74–177) and human PsLon (aa residues 2–328), respectively, which were liberated from GST-Tysnd1(N74–177) and GST-PsLon(N328), respectively, by cleavage with Prescission protease (Sigma). Antibodies to Tysnd1 and PsLon were purified by affinity chromatography using a CL-4B column (GE Healthcare) conjugated to GST-Tysnd1(N74–177) and GST-PsLon(N328), respectively, according to the manufacturer's instructions. The anti-human DBP antibody was raised in rabbits by injection of DNA encoding aa 282–381 of human DBP (19) using genomic antibody technology (Strategic Diagnostics, Newark, DE).

DNA Constructions—A cDNA encoding human Tysnd1 was amplified by reverse transcription-PCR (30) using mRNA from normal skin fibroblasts as the template and the primers HsTy-RTBamFw and HsTy-RTSalRv (supplemental Table S3). To construct *HA-* and *FLAG-Tysnd1-WT*, a BamHI-SalI fragment of the PCR product was inserted into pcDNAZeo3.1 (Invitrogen) by replacing the ubiquitin-containing fragment of pcDNAZeo/*HA_2-Ub* and pcDNAZeo/*FLAG-Ub*, respectively. For the construction of *HA-* and *FLAG*-tagged *Tysnd1-SA* encoding a protease-inactive mutant of Tysnd1 carrying a Ser^{481} to Ala substitution, two-step PCR (30) was carried out using two pairs of primers, HsTy-AxyFw plus HsTy-S481ARv and HsTy-S481AFw plus universal BGH primer. The amplified product was used to replace an AxyI-XbaI fragment of pcDNAZeo/*HA-* and *FLAG-Tysnd1-WT* to generate *HA-* and *FLAG*-tagged *Tysnd1-SA*, respectively. To construct *HA-Tysnd1-N* encoding aa 2–110 with an additional 5 aa (GGSKL) and *HA-Tysnd1-C* encoding aa 111–566, PCR was carried out using the primer pairs T7 plus HsTy-NRv and HsTy-CFw plus HsTy-566Rv, respectively. The BamHI-NotI fragment of each amplified product was inserted into pcDNAZeo3.1 as described for *HA-Tysnd1-WT*. To generate *HA-Tysnd1-ΔCv* encoding a Tysnd1 variant lacking 8 aa residues (aa 106–113), the BamHI-SpeI and SpeI-AxyI fragments of PCR products amplified using primers T7 plus HsTy-ΔCvRv and HsTy-ΔCvFw plus HsTy-AxyRv, respectively, were ligated together into pcDNAZeo3.1 as described above.

Human PsLon cDNA coding for human PsLon in pME18SFL3 (GenBank™ accession number AK074775) was provided by the National Institute of Technology and Evaluation Biological Resource Center (Kisarazu, Japan). To construct *HA-PsLon-WT*, PCR was carried out using the primers HsPsLon-dMBamFw and HsPsLon-HdRv. The BamHI-HindIII fragment of the amplified product and the HindIII-NotI fragment of pME18SFL3/*HsPsLon* were inserted together into pcDNAZeo3.1 as described for *HA-Tysnd1-WT*. The construction of *HA-PsLon-SA* encoding a protease-inactive PsLon mutant with a Ser^{743} to Ala substitution was similar to that of *HA-Tysnd1-SA* except that two-step PCR was carried out using the primer pairs HsPsLon-AxyFw and HsPsLon-S743ARv plus HsPsLon-S481AFw and universal BGH primer. To construct *GST-Tysnd1N(74–177)* and *GST-PsLonN328*, PCR was carried out using two primer pairs: HsTy-GSTN74Fw plus HsTy-GSTN177Rv and HsPsLon-GSTBamFw plus HsPsLon-GSTN328Rv, respectively. BamHI-NotI fragments of the amplified products were separately inserted into pGEX6P-1 (GE Healthcare).

To construct rat *FLAG-AOx*, the BglII-DraI fragment of a PCR product amplified using the primers RnAOx-BglFw and RnAOx-DraRv and the DraI-SacI fragment from pTZ19R/*RnAOx* (31) were ligated together into pUcD2Hyg/*FLAG-Rn-PEX12* (24) from which the *PEX12* fragment had been excised. A cDNA encoding human TH was amplified by RT-PCR as described for *Tysnd1* using the primers HsTH-BamRTFw and HsTH-XhoRTRv. To construct *TH-HA*$_2$, the BamHI-SalI fragment of the amplified PCR product was inserted into pcDNAZeo/*C-HA*$_2$. *FLAG-EGFP-SKL* was described previously (17). All of the sequences of the plasmid constructs were confirmed by nucleotide sequence analysis.

Blue Native PAGE—Blue native PAGE was performed as described previously (32) with minor modifications. Briefly, organelle fractions of HEK293 cells were solubilized on ice for 30 min with 1% digitonin in 1× native PAGE sample buffer (50 mM Bis-Tris, pH 7.2, 50 mM NaCl, 10% glycerol, 0.001% Ponceau S) (Invitrogen) and centrifuged at 20,000 × *g* for 30 min. Supernatant fractions were mixed with Coomassie Brilliant Blue G-250 at a final concentration of 0.25% before electrophoresis. Proteins were separated by electrophoresis on a 4–16% gradient Novex Bis-Tris gel (Invitrogen) at 4 °C for 1 h at 150 V and then for an additional 1.5 h at 250 V according to the manufacturer's protocol.

Subcellular Fractionation and Immunoprecipitation—To isolate immune complexes for mass spectroscopy, HEK293 cells stably expressing FLAG-Pex5pL or FLAG-Tysnd1 were homogenized with a Potter-Elvehjem Teflon homogenizer and fractionated as described previously (28). Organelle and cytosol fractions were lysed in buffer-L containing 20 mM Hepes-KOH, pH 7.4, 150 mM NaCl, 0.5% Triton X-100, 1 mM dithiothreitol, 1 mM EDTA, 5 μM MG132 (Peptide Institute, Osaka, Japan), and protease inhibitor mixture. Immunoprecipitation was carried out using anti-FLAG IgG-agarose (Sigma) as described (24). After washing the beads, proteins bound to the anti-FLAG IgG-agarose were eluted with buffer-L containing 100 μg/ml FLAG peptide (Sigma) and then subjected to analysis by mass spectroscopy (see below). Cells were also lysed directly in buffer-L, and the soluble fractions were subjected to immunoprecipitation and immunoblot analysis. Endogenous Tysnd1 and PsLon in HEK293 cells were isolated by immunoprecipitation for 2 h at 4 °C with their respective rabbit antiserum or their purified IgG and Protein A-Sepharose beads (GE Healthcare). Co-immunoprecipitated proteins were analyzed by SDS-PAGE and immunoblot as described previously (24).

Mass Spectroscopy—FLAG eluates of anti-FLAG-Pex5pL and anti-FLAG-Tysnd1-SA immunoprecipitates were resolved by SDS-PAGE and stained separately with Coomassie Brilliant Blue G-250 (Nacalai Tesuque, Kyoto, Japan) or silver stain with a Sil-Best stain kit (Nacalai Tesque), respectively. For FLAG-Pex5pL, lanes containing immunoprecipitates from cytosol and organelle fractions were cut into 36 slices. For FLAG-Tysnd1-SA, sliver-stained protein bands were excised along with the same regions of control gel slices containing immunoprecipitates from untransfected HEK293 cells. Following in-gel reduction, alkylation, and digestion with trypsin, proteins were analyzed by an ion trap mass spectrometer (LCQ-Deca, Finnigan) equipped with a nano-LC electrospray ionization source at the Post-genome Research Center of Kyushu University as described previously (33). Collision-induced dissociation spectra were acquired automatically in the data-dependent scan mode with a dynamic exclusion option and were compared with human entries in the International Protein Index (European Bioinformatics Institute) using the Mascot algorithm. Assigned high scoring peptide sequences (Mascot score >40) were manually confirmed by comparison with the corresponding collision-induced dissociation spectra.

Immunofluorescence Microscopy—Immunostaining of cells was performed as described previously (24) using 4% paraformaldehyde for cell fixation and 0.1% Triton X-100 for permeabilization. Immune complexes were visualized using Alexa Fluor 488- or 568-labeled goat anti-rabbit or anti-mouse IgG antibody (Invitrogen). Cells were observed using a confocal laser microscope (LSM510; Carl Zeiss) equipped with a Plan Apochromat 100×/1.4 numerical aperture oil immersion objective lens and argon and dual HeNe lasers. Images were acquired with an LSM image browser (Carl Zeiss), and images were prepared using Adobe Photoshop CS4.

Small Interfering RNA (siRNA)—Knockdown of Tysnd1 and PsLon in HeLa cells was performed using Stealth siRNA duplexes (Invitrogen). The target sequences of the siRNAs were as follows: human *Tysnd1-1*, 5′-UACGGUGCCGCACUCCACCAACACU-3′; human *Tysnd1-2*, 5′-UCCUGACUGGCAAAUACCACACGGC-3′; human *PsLon-1*, 5′-UGUACAAUCUGGAAACGGCAUAGGC-3′; human *PsLon-2*, 5′-AUCUCUUUGACACAGACUUUAUGGG-3′; and human *PEX5*, 5′-GGCAGAGAATGAACAAGAACTATTA-3′. Stealth RNAi Negative Control (Invitrogen) was used as a control. HeLa cells were transfected twice at a 48-h interval with 33 nM siRNA and Lipofectamine 2000 as described (34).

Measurement of β-Oxidation Activity—The fatty acid β-oxidation assay was performed essentially as described previously (35). HeLa cells cultured in 12-well dishes were preincubated at 37 °C for 1 h in serum-free DMEM. After the medium was changed to 0.4 ml of fresh serum-free DMEM, the fatty acid β-oxidation reaction was initiated by adding 2 nmol of 1-^{14}C-labeled lignoceric acid (American Radiolabeled Chemicals) conjugated to 10 mM α-cyclodextrin (Sigma) dissolved in 0.1 ml of 100 mM Tris-HCl, pH 8.0. After incubation for 2 h at 37 °C, the reactions were terminated on ice for 30 min by adding 75 μl of 10% FCS-supplemented DMEM and 0.1 ml of 3.0 M perchloric acid. The reaction mixtures were centrifuged to remove cell debris, and the resulting supernatants were extracted four times with hexane. Acid-soluble radioactivity was measured using a Beckman LS6500 liquid scintillation counter. Samples were prepared in quadruplicate; three of the four samples were used for the fatty acid β-oxidation assay, and the fourth was used for protein quantification with a protein assay kit (Bio-Rad). Fatty acid β-oxidation activity was expressed as pmol/min/μg of protein. Statistical significance was assessed by the unpaired Student's *t* test and is indicated as follows: *, $p < 0.05$; and **, $p < 0.01$.

RESULTS

Tysnd1 and PsLon Are Pex5p-binding Proteins—Pex5p is a cytosolic PTS1 receptor that plays a central role in peroxisome

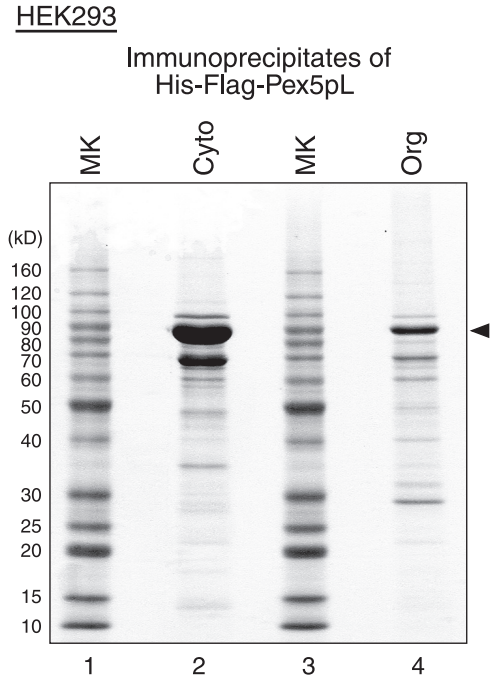

FIGURE 1. **Identification of Pex5p-interacting proteins.** The postnuclear supernatant fraction from HEK293 cells expressing His-FLAG-Pex5pL, termed HEK/HF-P5L, was separated into cytosol (*Cyto*; *lane 2*) and organelle (*Org*; *lane 4*) fractions. Both fractions were solubilized in buffer containing 0.5% Triton X-100 and subjected to immunoprecipitation using an anti-FLAG antibody conjugated to agarose beads. Immunoprecipitates were eluted with an excess of FLAG peptide and analyzed by SDS-PAGE and Coomassie Brilliant Blue staining. Purified FLAG-Pex5pL (*solid arrowhead*) and co-precipitated bands were in-gel digested and analyzed by LC-MS/MS. Molecular mass markers (*MK*) were loaded in *lanes 1* and *3*.

matrix protein import. Pex5p binds multiple partners, including cargo PTS1 proteins, via its C-terminal tetratricopeptide repeats, and Pex14p and Pex13p, two components of putative peroxisome import machinery, via the N-terminal region (8, 9). To gain mechanistic insight into peroxisome biogenesis, we used a proteomics-based approach to identify Pex5p-interacting proteins. Clonal HEK293 cells stably expressing His- and FLAG-tagged Pex5pL (His-FL-Pex5pL), termed HEK/HF-P5L, were established. His-FL-Pex5pL was isolated by immunoprecipitation using anti-FLAG IgG-agarose from separate cytosol and organelle fractions, and then the immunoprecipitates were separated by SDS-PAGE. FL-Pex5pL was mainly detected in the cytosol fraction, migrating with an apparent molecular mass of 90 kDa, and only partly in the organelle fraction (Fig. 1, *arrowhead*), consistent with results from earlier studies on the distribution of endogenous Pex5p in CHO cells and human fibroblasts (15, 36). All of the discernible bands in each lane were excised and trypsinized, and the resulting peptides were analyzed by LC-MS/MS as described under "Experimental Procedures." Of the 19 PTS1-containing proteins identified, nine were enzymes, including proteins involved in peroxisomal fatty acid β-oxidation and two proteins that contained serine protease domains, Tysnd1 (21) and PsLon (23) (supplemental Table S1). Furthermore, the PTS2 receptor Pex7p and five membrane peroxins, Pex14p, Pex13p, and the three RING peroxins Pex2p, Pex10p, and Pex12p, were also identified (supplemental Table S1) in good agreement with earlier reports (15, 17). We next investigated the functional roles of Tysnd1 and PsLon, both of which harbor a unique serine protease-like domain, in peroxisomes.

Detection of Endogenous Tysnd1 and PsLon—Human Tysnd1 and PsLon cDNAs, encoding proteins of 566 and 852 aa, respectively, were cloned. Both proteins had a typical PTS1 tripeptide (Ser-Lys-Leu-COOH) at their C terminus (Fig. 2*A*). Tysnd1 contained a serine protease-like domain that has been shown to be responsible for the proteolytic processing of several PTS1 and PTS2 proteins (21). Self-cleavage of Tysnd1 between aa 110 and 111 into N- and C-terminal fragments (Fig. 2*A*, *arrowhead*) was observed (see Fig. 4*B*, *lane 2*) as reported previously(21). The domain structure of PsLon was similar to that of ATP-dependent Lon protease family members, containing an AAA (ATPases associated with diverse cellular activities) domain and a serine protease domain (Fig. 2*A*) (22, 23).

Rabbit polyclonal antibodies raised against aa residues 74–177 of Tysnd1 and 2–328 of PsLon (Fig. 2*A*, *underlines*) were assessed by immunoprecipitation and immunoblot experiments. The anti-Tysnd1 antibody specifically recognized and immunoprecipitated 60- and 45-kDa bands, corresponding to endogenous full-length Tysnd1 and the C-terminal cleavage fragment (Tysnd1-C), respectively, with similar efficiency in HEK293 cell lysates (Fig. 2*B*, *upper panel*, *lanes 1–3*), whereas no bands were detectable in immunoprecipitates derived using preimmune serum (*lane 4*). The N-terminal 10-kDa cleavage fragment of Tysnd1 (Tysnd1-N) containing aa 74–111 was below the level of detection in HEK293 cells presumably due to instability in peroxisomes (described below) as well as lower reactivity of the anti-Tysnd1 antibody toward Tysnd1-N (data not shown). The anti-PsLon antibody recognized and specifically immunoprecipitated endogenous 90-kDa PsLon (Fig. 2*B*, *lower panel*, *lanes 5–7*).

Immunostaining of HEK293 cells with an anti-Tysnd1 antibody revealed numerous punctate structures that co-localized with catalase, a peroxisomal matrix marker protein, strongly suggesting that Tysnd1 localizes to peroxisomes (Fig. 2*C*, *panels a–c*). Immunostaining of HEK293 cells with an anti-PsLon antibody revealed numerous particles that were superimposable on Pex14p-positive peroxisomes (Fig. 2*C*, *panels d–f*), indicating that PsLon also localizes to the peroxisome. Subtle nuclear staining with the anti-PsLon antibody was most likely nonspecific as a similar pattern of staining of cell nuclei was detected with preimmune serum (data not shown).

Tysnd1 Is Required for Proteolytic Processing of Peroxisomal Fatty Acid β-Oxidation Enzymes—The putative role of Tysnd1 and PsLon in the regulation of peroxisomal fatty acid β-oxidation was assessed by RNA interference targeting Tysnd1 and PsLon in HeLa cells. Endogenous Tysnd1 in HeLa cells was detectable in control siRNA-transfected cells in two forms, a predominant 60-kDa form, termed Tysnd1-F, and a less abundant 45-kDa form, termed Tysnd1-C (Fig. 3*A*, *lane 1*). In HeLa cells transfected with *Tysnd1-1* and *-2* siRNAs, Tysnd1 was barely detectable (Fig. 3*A*, *lanes 2* and *3*), indicative of the efficient depletion of Tysnd1. Similarly, the levels of PsLon and the PTS1 receptor Pex5p were reduced to below the level of detection in HeLa cells transfected with their respective siRNAs (Fig. 3*A*, *lanes 4–6*). AOx, a PTS1-containing enzyme, is synthesized as 75-kDa A-chain (AOx-A) that is converted to 53-kDa AOx-B

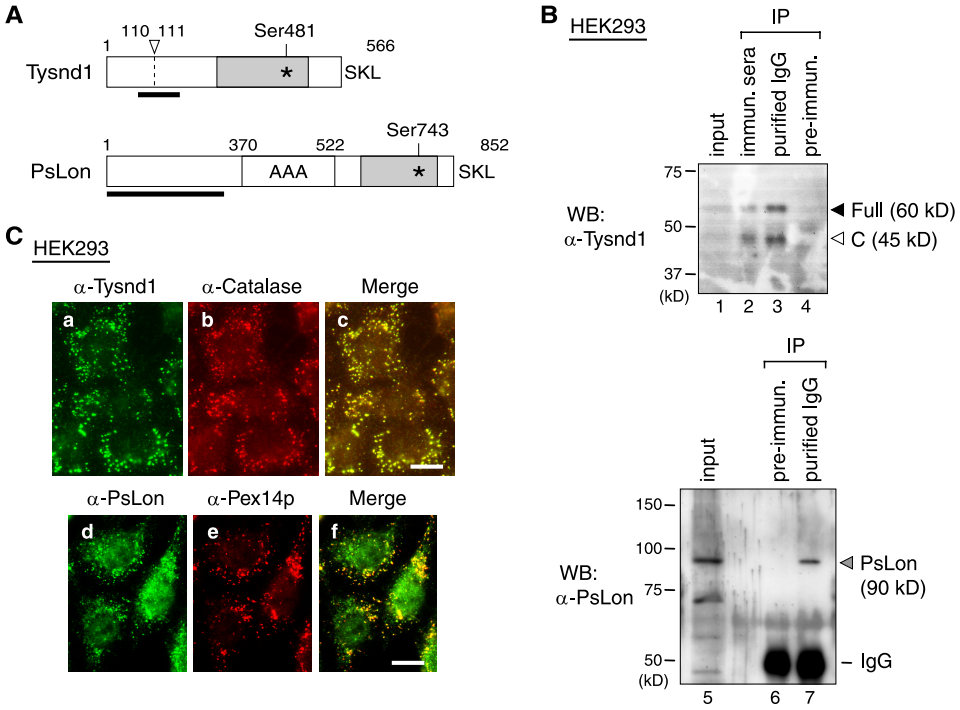

FIGURE 2. **Tysnd1 and PsLon are serine protease domain-containing peroxisomal proteins.** *A*, schematic representation of the domain structure of Tysnd1 and PsLon. *Asterisks* indicate Ser^{481} and Ser^{743}, putative active site residues in the serine protease domains (*gray boxes*) of Tysnd1 and PsLon, respectively. The *arrowhead* indicates the self-cleavage site of Tysnd1 (21). *Solid underlines* indicate the regions used to raise rabbit antibodies to human Tysnd1 (residues 74–177) and PsLon (residues 2–328). *AAA*, AAA superfamily of ATPases. *B*, SDS-PAGE and immunoblot analysis of endogenous Tysnd1 and PsLon. Endogenous Tysnd1 and PsLon were immunoprecipitated from HEK293 cell lysates using the indicated antisera (*lanes 2* and *6*) or purified IgG (*lanes 3* and *7*). Tysnd1 preimmune (*pre-immun.*) serum was also assessed (*upper panel*, *lane 4*). *Input*, 5% of the total lysate used for immunoprecipitation (*IP*) (*lanes 1* and *5*). *Solid*, *open*, and *gray arrowheads* indicate full-length Tysnd1 (*Full*), the self-cleaved C-terminal region of Tysnd1 encompassing residues 111–566 (*C*), and PsLon, respectively. *IgG*, immunoglobulin G heavy chain. *C*, Tysnd1 and PsLon were visualized by immunofluorescence microscopy. HEK293 cells were co-immunostained with antibodies to Tysnd1 (*panel a*) plus catalase (*panel b*) and PsLon (*panel e*) plus Pex14p (*panel f*). Merged views are presented in *panels c* and *f*. *Scale bars*, 10 μm. *WB*, Western blot.

and 22-kDa AOx-C fragments by intraperoxisomal processing (31). Full-length 79-kDa DBP and the 59-kDa SCPx precursor PTS1 enzymes that catalyze the second/third steps and the last step, respectively, in the peroxisomal fatty acid β-oxidation pathway are likewise converted to proteolytic fragments in peroxisomes: DBP is converted into 35-kDa N- and 44-kDa C-terminal fragments (20), whereas the SCPx precursor is converted into 46-kDa N- and 13-kDa C-terminal fragments (26, 37). In cells treated with *Tysnd1* siRNAs, full-length AOx-A, DBP, and the SCPx precursor were significantly elevated, correlating with decreased levels of Tysnd1 (Fig. 3*A*, *lanes 2* and *3*). The PTS2-containing larger precursor of TH is proteolytically processed to the mature enzyme in peroxisomes (6, 7). Likewise, the PTS2 presequence of alkyldihydroxyacetonephosphate synthase (38), the second step enzyme in plasmalogen synthesis, is processed to generate the mature protein in peroxisomes (27). TH and alkyldihydroxyacetonephosphate synthase precursors were readily detectable by immunoblot in *Tysnd1-2* siRNA-treated HeLa cells (Fig. 3*A*, *lane 3*), strongly suggesting that Tysnd1 is responsible for PTS2 cleavage as well as processing of PTS1-containing proteins. In *Tysnd1-2* siRNA-treated HeLa cells, AOx was detectable by immunostaining in numerous peroxisomes as seen in the merged view with Pex14p staining (Fig. 3*B*, *panels b*, *e*, and *h*) similar to cells treated with control siRNA (Fig. 3*B*, *panels a*, *d*, and *g*). Peroxisomal localization of alkyldihydroxyacetonephosphate synthase and catalase was also apparent in Tysnd1-depleted HeLa cells (data not shown), suggesting that Tysnd1 is not essential for the import of matrix proteins into peroxisomes. Interestingly, knockdown of Tysnd1, but not PsLon, resulted in morphological changes of the peroxisome to an elongated shape (Fig. 3*B*, *panels j–l*) similar to what has been observed in AOx- and DBP-deficient fibroblasts (39), implying a functional relationship between Tysnd1 and peroxisomal fatty acid β-oxidation. The phenotypes of the precursor proteins in *Tysnd1* siRNA-treated cells were distinct from that observed in *PEX5* siRNA-treated cells in which AOx, TH, and alkyldihydroxyacetonephosphate synthase were eliminated, and there was a severe reduction of Tysnd1 and PsLon mostly likely due to impaired import of peroxisomal matrix proteins and consequent degradation in the cytosol (Fig. 3*A*, *lanes 2*, *3*, and *6*). Collectively, these results strongly suggested that Tysnd1 is a *bona fide* proteolytic processing enzyme for endogenous PTS1 and PTS2 precursor proteins *in vivo*, consistent with results obtained previously using ectopically expressed Tysnd1 and substrate proteins in COS7 cells (21).

By contrast, knockdown of PsLon had little effect on peroxisomal localization of AOx, peroxisome morphology (Fig. 3*B*, *panels c*, *f*, *i*, and *l*), and proteolytic processing of PTS1 and PTS2 enzymes. Tysnd1-C, but not full-length Tysnd1 or the N-terminal fragment of DBP, was modestly stabilized (Fig. 3*A*, *lanes 4* and *5*). These results suggested that PsLon is not directly involved in the processing of peroxisomal fatty acid β-oxidation enzymes.

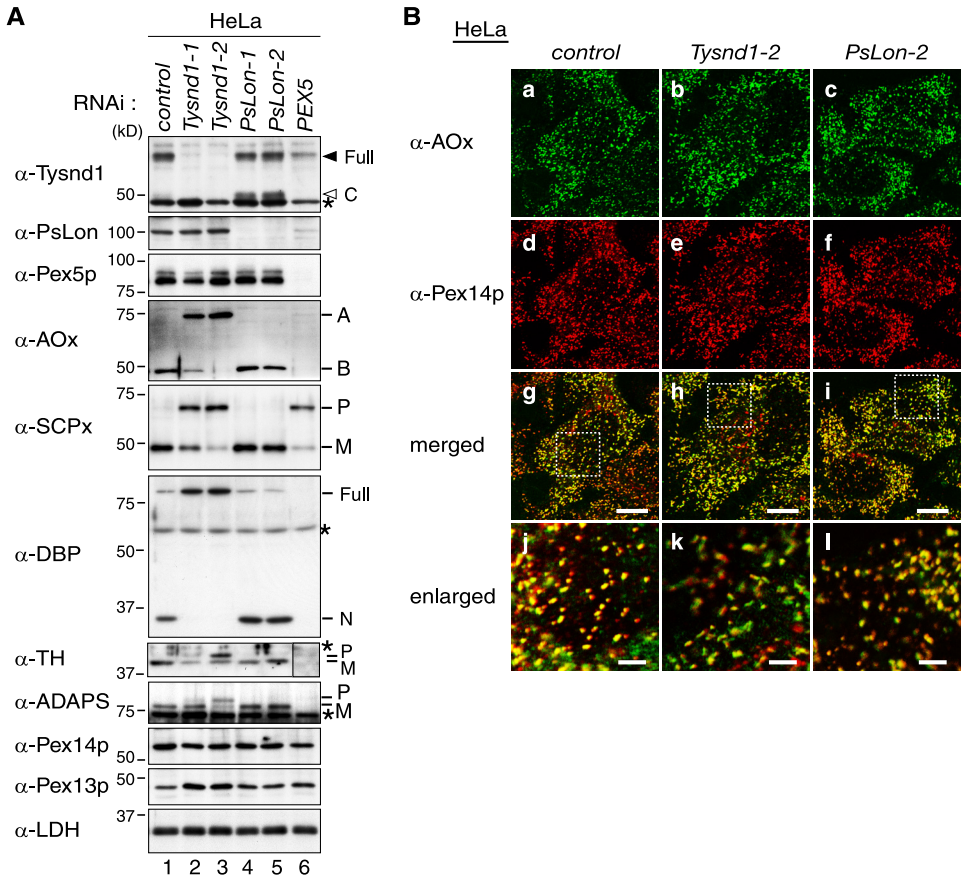

FIGURE 3. **Knockdown of Tysnd1, but not PsLon, abrogates proteolytic processing of peroxisomal fatty acid β-oxidation enzymes.** *A*, HeLa cells were transfected twice at a 48-h interval with a control siRNA (*lane 1*), two independent siRNAs specific for Tysnd1 (*lanes 2* and *3*) and PsLon (*lanes 4* and *5*), and a *PEX5* siRNA (*lane 6*). Forty-eight hours after the second transfection, cells were lysed and analyzed by SDS-PAGE and immunoblot using the antibodies indicated on the *left*. *LDH*, lactate dehydrogenase. *Asterisks* indicate nonspecific bands. *A* and *B*, components A and B of AOx; *P* and *M*, precursor and mature forms, respectively. *B*, HeLa cells were transfected with a control siRNA (*panels a*, *d*, *g*, and *j*), *Tysnd1* siRNA (*Tysnd1-2*) (*panels b*, *e*, *h*, and *k*), and *PsLon* siRNA (*PsLon-1*) (*panels c*, *f*, *i*, and *l*). Cells were subjected to immunostaining using antibodies for AOx (*panels a–c*) and Pex14p (*panels d–f*). *Boxed* areas in the merged views (*panels g–i*) are enlarged in *panels j–l*. *Scale bars*, 10 μm (*panels a–i*) and 2.5 μm (*panels j–l*). Note that the peroxisomes in cells treated with *Tysnd1-2* siRNA were elongated as compared with cells treated with *PsLon-1* siRNA. *ADAPS*, alkyldihydroxyacetonephosphate synthase.

Self-cleavage of Tysnd1 Regulates Its Proteolytic Processing Activity—To determine whether self-cleavage of Tysnd1 altered its proteolytic activity, ectopic expression and analysis of various Tysnd1 mutants tagged with HA were carried out (Fig. 4*A*). In CHO-K1 cells, wild-type (WT) HA-Tysnd1 and all of the mutants co-localized with Pex14p in peroxisomes (supplemental Fig. S1) similarly to endogenous Tysnd1 (Fig. 2*C*). There were relatively fewer cells expressing HA-Tysnd1-N, consistent with the results of immunoblot analysis suggesting that the N-terminal fragment of Tysnd1 is unstable (Fig. 4*B*, *lane 4*). Upon expression of HA-Tysnd1-WT in CHO-K1 cells, both the 46- and 15-kDa bands corresponding to Tysnd1-C and -N, respectively, were detected by immunoblot in addition to the 62-kDa full-length form (Fig. 4*B*, *lane 2*). In cells expressing HA-Tysnd1-SA, which contained a Ser^{481}-to-Ala substitution in the putative active site, no processed fragments were detected, strongly suggesting that the S481A mutation abrogated the self-cleaving activity of Tysnd1 (Fig. 4*B*, *lane 3*). HA-Tysnd1-ΔCv-WT in which the 8 aa surrounding the self-cleavage site between Cys^{110} and Ala^{111} were deleted (Fig. 4*A*, *arrowhead*) (21) and the corresponding SA mutant, HA-Tysnd1-ΔCv-SA, were also detectable only as full-length proteins, indicating that these mutants were resistant to self-cleavage (Fig. 4*B*, *lanes 7* and *8*). HA-Tysnd1-C-WT and the HA-Tysnd1-C-SA mutant were likewise detected at similar levels as intact 50-kDa proteins (Fig. 4*B*, *lanes 5* and *6*).

To further investigate the mechanism of self-cleavage of Tysnd1, HA-Tysnd1 variants with protease activity were co-expressed in CHO-K1 cells together with a FLAG-tagged protease inactive form of Tysnd1, FL-Tysnd1-SA (Fig. 4*C*, *upper panels*). In mock-transfected cells or cells co-transfected with HA-Tysnd1-SA or a control PTS1 protein (EGFP-SKL), FL-Tysnd1-SA was detected only as the 62-kDa full-length protein (Fig. 4*C*, *upper panels*, *lanes 1*, *3*, and *9*), indicating that FL-Tysnd1-SA and HA-Tysnd1-SA were indeed defective in self-cleaving activity as noted (Fig. 4*B*, *lane 3*). FL-Tysnd1-SA was cleaved into Tysnd1-C upon co-expression with HA-Tysnd1-WT and HA-Tysnd1-ΔCv-WT but not their corresponding SA variants, HA-Tysnd1-C-WT, and HA-Tysnd1-C-SA (Fig. 4*C*, *upper panels*, *lanes 2* and *5–8*). These results suggested that only full-length Tysnd1 catalyzes intermolecular self-cleavage and that this leads to down-regulation of Tysnd1 protease activity.

The proteolytic processing activity of HA-Tysnd1 variants toward other peroxisomal substrates such as the PTS1 enzyme AOx and the PTS2 protein TH was also examined. In contrast

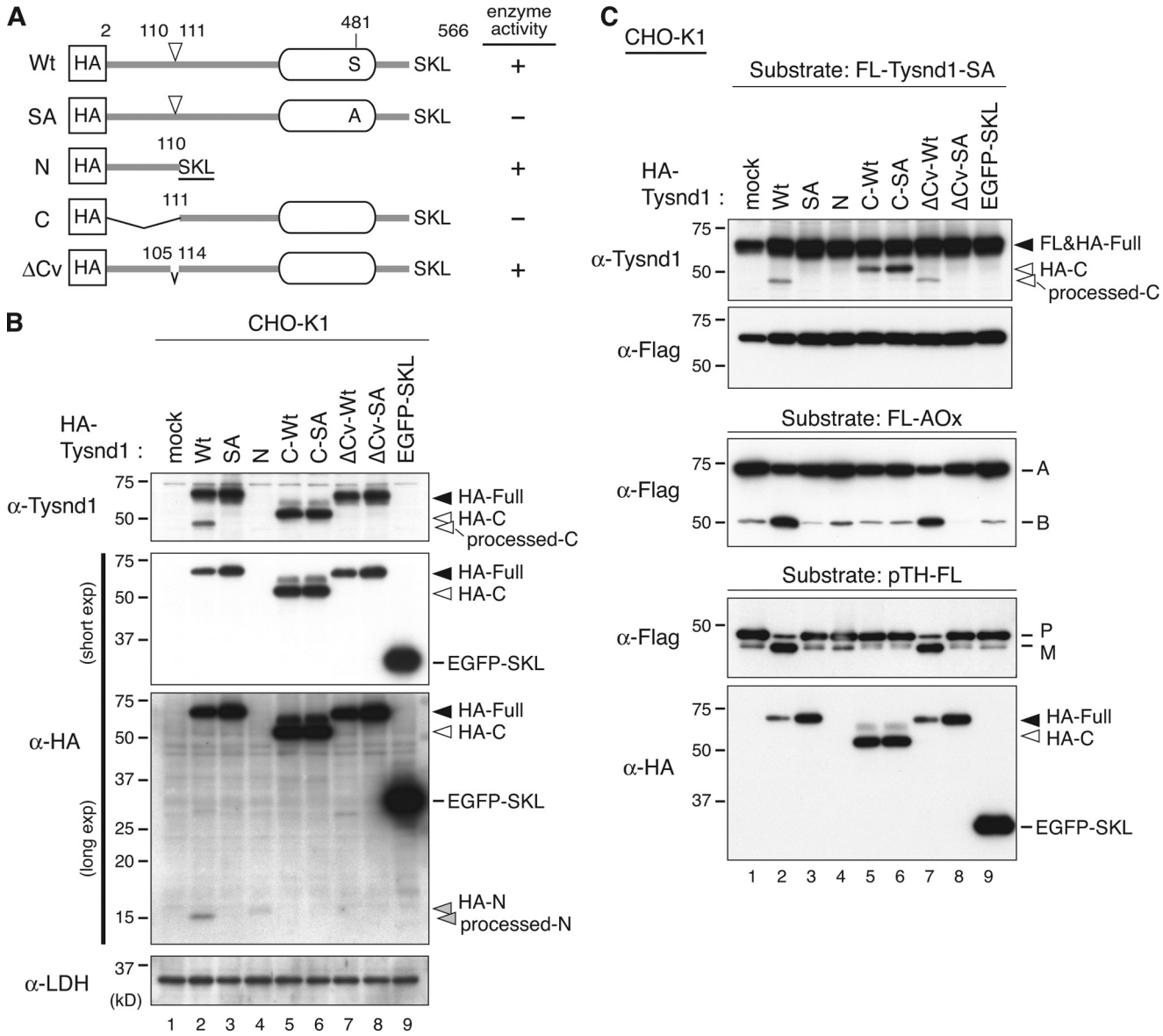

FIGURE 4. **Full-length but not processed N- and C-terminal regions of Tysnd1 exhibits proteolytic activity against AOx and TH.** *A*, schematic representation of the N-terminal HA-tagged Tysnd1 variants used in this study. The *rounded box* shows the serine protease domain. *S* and *A* designate Ser^{481} and the Ser^{481}-to-Ala mutation in the active site of WT Tysnd1 and the SA mutant, respectively. Tysnd1 variants *N* and *C* represent the N-terminal region encompassing residues 2–110 with an additional PTS1 signal (5 aa; -GGSKL) and the C-terminal region consisting of residues 111–566, respectively. The ΔCv variant of Tysnd1 lacks the 8 aa (residues 106–113) surrounding the self-cleavage site located between Cys^{110} and Ala^{111} (*arrowhead* at the *top*) (21). *B*, self-cleavage of Tysnd1 variants. CHO-K1 cells were co-transfected with plasmids encoding the indicated HA-Tysnd1 variants and HA-EGFP-SKL or a mock plasmid. After 24 h, cells were lysed and analyzed by SDS-PAGE and immunoblot using anti-Tysnd1 and -HA antibodies. *Solid*, *open*, and *gray arrowheads* indicate full-length Tysnd1 and the C- and N-terminal cleavage products, respectively. *C*, self-cleaving and processing activity toward AOx and TH of Tysnd1 variants. CHO-K1 cells were transfected with plasmids encoding the indicated HA-Tysnd1 variants as in *B* together with plasmids encoding FL-Tysnd1-SA (*top panels*), FL-AOx (*middle panels*), and TH-FL (*lower panels*) (DNA ratio at 1:2.5). After 24 h, cells were lysed and analyzed by SDS-PAGE and immunoblot using anti-Tysnd1, -FLAG, and -HA antibodies. *Solid* and *open arrowheads* indicate epitope-tagged full-length and C-terminal Tysnd1, respectively. *LDH*, lactate dehydrogenase; *exp*, exposure. *A* and *B*, components A and B of AOx; *P* and *M*, precursor and mature forms, respectively.

to endogenous AOx, which is present mostly as AOx-B in CHO-K1 (25) and HeLa cells (Fig. 3*A*, *lane 1*), FLAG-tagged AOx (FL-AOx) was detected predominantly as the 75-kDa FL-AOx-A form, and detected at a much lower level was the 52-kDa FL-AOx-B form, which is presumably the proteolytic product of conversion of the A form by endogenous Tysnd1 (Fig. 4*C*, *middle panel*, *lane 1*). Co-expression of Tysnd1-WT and Tysnd1-ΔCv-WT resulted in significantly lower levels of FL-AOx-A and increased levels of FL-AOx-B, indicative of the proteolytic activity of the Tysnd1 proteins (Fig. 4*C*, *middle panel*, *lanes 2* and *7*). A lower level of AOx-B was also detected in mock-transfected cells and cells expressing Tysnd1-N, -C-WT, -C-SA, or EGFP-SKL (Fig. 4*C*, *middle panel*, *lanes 1*, *4–6*, and *9*). Interestingly, FL-AOx-B was barely detectable in cells that co-expressed Tysnd1-SA and -ΔCv-SA (Fig. 4*C*, *middle panel*, *lanes 3* and *8*), suggesting that these two SA mutants functioned in a dominant-negative manner to inhibit endogenous Tysnd1. When we examined the processing of a PTS2-containing substrate, namely the larger precursor of peroxisomal thiolase tagged with a C-terminal FLAG tag (TH-FL), the PTS2 presequence was cleaved only when TH-FL was co-ex-

pressed with HA-Tysnd1-WT and -ΔCv-WT (Fig. 4*C*, *lower panels*, *lanes 2* and *7*). Together, these results strongly suggested that the active form of Tysnd1 in processing heterologous substrates such as AOx and TH is the full-length form of the protein. Moreover, proteolytic processing of substrates by Tysnd1 for the most part occurred only when the substrates were located in peroxisomes as verified by immunostaining (data not shown). These results confirmed that the processing reaction takes place in peroxisomes. Thus, full-length Tysnd1 appears to be the active form of the enzyme in the proteolytic processing of PTS1 and PTS2 proteins and in self-cleavage, and intermolecular self-cleavage of Tysnd1 down-regulates its protease activity.

Tysnd1 Forms Distinct Oligomers and Interacts with PsLon—To further investigate the function of Tysnd1 in peroxisomes, LC-MS/MS was used to identify proteins that co-immunoprecipitated with Tysnd1 from cells. An organelle fraction from HEK293 cells stably expressing protease-inactive FL-Tysnd1-SA was subjected to immunoprecipitation using anti-FLAG IgG-agarose followed by SDS-PAGE and silver staining (Fig. 5*A*). Several proteins were specifically co-immunoprecipitated with FL-Tysnd1-SA. Two proteins of 50 and 80 kDa were identified as AOx B and DBP, respectively; both are substrates of Tysnd1 (Ref. 21 and this study) (Fig. 5*A*, *lanes 2* and *3*). Two proteins of 45 and 38 kDa were also identified as DBP (Fig. 5*A*, *bands 2*, *4*, and *6*) and were presumably the result of peroxisomal processing (20) or degradation during immunoprecipitation. Furthermore, PsLon, peroxisomal *trans*-enoyl-CoA isomerase, and nonspecific lipid transfer protein (also called sterol carrier protein 2) were also identified (Fig. 5*A*, *lane 3*). Immunoblot analysis of anti-FL-Tysnd1-SA immunoprecipitates from an HEK293 cell line stably expressing FL-Tysnd1-SA revealed the presence of AOx-B and PsLon, providing further support that these proteins indeed interact with Tysnd1. In another HEK293 cell line stably expressing FL-Tysnd1-WT, AOx-B and PsLon were barely detectable (Fig. 5*B*, *left panel*). The precursor of SCPx, another PTS1 substrate of Tysnd1 (Ref. 21 and this study), was also co-immunoprecipitated preferentially with FL-Tysnd1-SA but was barely detectable in FL-Tysnd1-WT immunoprecipitates, whereas a very low amount of the mature form of SCPx was co-immunoprecipitated with both forms of FL-Tysnd1 (Fig. 5*B*, *right panel*). By contrast, the PTS2 substrates TH and alkyldihydroxyacetonephosphate synthase did not co-immunoprecipitate with FL-Tysnd1-WT or FL-Tysnd1-SA (Fig. 5*B*), which suggested that there may be different mechanisms of recognition of PTS1 and PTS2 proteins by Tysnd1. In anti-FL-Tysnd1-WT and -FL-Tysnd1-SA immunoprecipitates, the Tysnd1-C fragment (apparently the result of self-cleavage) and endogenous Tysnd1, respectively, were present at nearly the same levels, suggesting that full-length Tysnd1 interacts with the self-cleaved Tysnd1-C (Fig. 5*B*, *right panel*, *lanes 5* and *6*).

To determine whether Tysnd1 forms oligomers, the ΔCv-WT and C-WT variants of FL-Tysnd1 were co-expressed with HA-Tysnd1 and its variants in HeLa cells (Fig. 5*C*). HA-Tysnd1-C-WT and HA-Tysnd1-ΔCv-WT were specifically co-immunoprecipitated with FL-Tysnd1-ΔCv-WT (Fig. 5*C*, *lanes 10–15*) in agreement with the results in Fig. 5*B* (*right panel*, *lanes 4–6*). Moreover, HA-Tysnd1-C-WT was present at higher levels in the immunoprecipitates compared with HA-Tysnd1-ΔCv-WT (Fig. 5*C*, *lanes 16–18*). These results suggested that Tysnd1 forms distinct oligomeric complexes consisting of full-length protein, full-length protein bound to the C-terminal cleavage product, and oligomers of the C-terminal fragment similar to what has been reported for AOx complexes consisting of heteromeric dimers (A_2, ABC, and B_2C_2) (40). Endogenous PsLon in HeLa cells was also preferentially co-immunoprecipitated with FL-Tysnd1-C-WT compared with FL-Tysnd1-ΔCv-WT (Fig. 5*C*, *lanes 13–18*), confirming the interaction between Tysnd1 and PsLon.

In HEK293 stable cell lines expressing FL-Tysnd1-WT or FL-Tysnd1-SA, two distinct 160-kDa and 120-kDa proteins that were recognized by both anti-FLAG and anti-Tysnd1 antibodies were identified by blue native PAGE in organelle fractions (Fig. 5*D*, *lanes 1–9*, *solid* and *open arrowheads*). Two other bands with masses of 220 and ~60 kDa were also discernible (Fig. 5*D*). Endogenous Tysnd1 was mainly detected in the 120- and 60-kDa bands in HEK293 cells (Fig. 5*D*, *lane 7*). Because Tysnd1 and FLAG-Tysnd1 migrated with a molecular mass of ~60 kDa in SDS-PAGE and only full-length FL-Tysnd1 was recognized by the anti-FLAG antibody (Figs. 2*B* and 5*B*), the prominent 160-kDa band detected by the anti-FLAG antibody was most likely a trimer of full-length FL-Tysnd1, and the 220-, 120-, and 60-kDa bands likely represented tetramers, dimers, and monomers of FLAG-tagged Tysnd1 or the SA mutant, respectively. FL-Tysnd1-WT and FL-Tysnd1-SA exhibited similar oligomeric compositions with oligomers of the same apparent migration in blue native PAGE analysis (Fig. 5*D*, *lanes 2* and *3*). By contrast, in SDS-PAGE, Tysnd1-WT comprised a mixture, including full-length forms as well as processed forms in nearly equal ratios, and Tysnd1-SA was present almost exclusively in the full-length form (Fig. 5*B*, *right panels*, *lanes 2* and *3*). These results strongly suggested that Tysnd1 oligomers initially contain the self-cleaved N- and C-terminal fragments of Tysnd1. Taken together, these results suggested that Tysnd1 forms hetero-oligomers of distinct molecular combinations and interacts with PTS1 substrates and PsLon in peroxisomes.

PsLon Preferentially Degrades Processed Forms of Tysnd1—To determine whether Tysnd1 served as a substrate of PsLon, wild-type HA-Tysnd1 and the corresponding N- and C-WT fragments were separately expressed in *PsLon-1* siRNA-treated HeLa cells in which endogenous PsLon was efficiently eliminated (Fig. 6*A*, *top panel*, *lane 5*). The levels of Tysnd1-N and -C fragments derived from HA-Tysnd1-WT were elevated in *PsLon-1* siRNA-transfected cells compared with control siRNA-treated cells (Fig. 6*A*, *middle panels*, *lanes 2* and *6*). HA-Tysnd1-C-WT was also detected at a somewhat higher level in PsLon-knocked down cells (Fig. 6*A*, *middle panels*, *lanes 3* and *7*). Endogenous Tysnd1-C was likewise detectable in cells expressing HA-Tysnd1-N and HA-Tysnd1-C-WT (Fig. 6*A*, *middle panels*, *lanes 3*, *4*, *7*, and *8*) as well as in mock-transfected cells (*lanes 1* and *5*). By contrast, the expression levels of full-length HA-Tysnd1-WT and endogenous Tysnd1 were not altered in PsLon-knocked down cells (Fig. 6*A*, *lanes 5–8*), strongly suggesting that PsLon is involved in the regulation of Tysnd1-N and -C fragments.

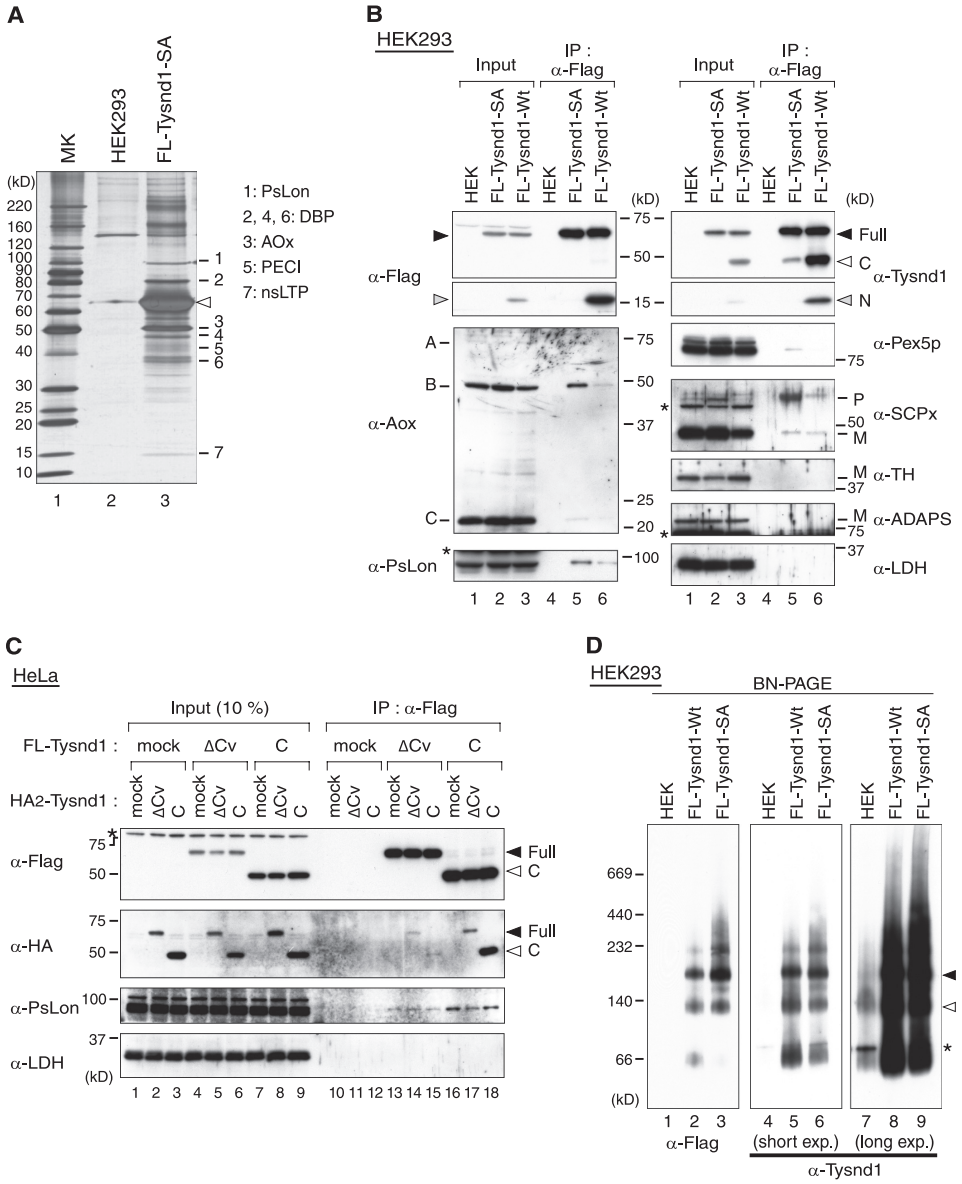

FIGURE 5. **Tysnd1 interacts with its substrates and PsLon.** *A*, identification of Tysnd1-binding proteins. Organelle fractions from HEK293 cells stably expressing FLAG-Tysnd1-SA and control HEK293 cells were subjected to immunoprecipitation using anti-FLAG IgG-conjugated agarose as described for Fig. 1. Proteins were separated by SDS-PAGE and visualized by silver staining. FLAG-Tysnd1-SA (*arrowhead*) and co-precipitated protein bands were in-gel digested and analyzed by LC-MS/MS as in Fig. 1. Identified proteins are listed on the *right*. *PECI*, peroxisomal *trans*-enoyl-CoA isomerase. *B*, immunoblot analysis of Tysnd1-interacting proteins. Wild-type (*lanes 3* and *6*) and SA mutant (*lanes 2* and *5*) forms of FLAG-Tysnd1 were isolated from the respective stable transformants of HEK293 cells by immunoprecipitation using anti-FLAG IgG-conjugated agarose as described for *A*. As a negative control, normal HEK293 cells were also subjected to immunoprecipitation (*lanes 1* and *4*). Immunoprecipitates were analyzed by SDS-PAGE and immunoblot using the indicated antibodies. *Input*, 10% of the total cell lysate used in each immunoprecipitation (*IP*). *Solid*, *open*, and *gray arrowheads* indicate FLAG-Tysnd1-F, -C, and -N, respectively. *P* and *M*, precursor and mature forms, respectively. *C*, the C-terminal cleavage product of Tysnd1 (Tysnd1-C) preferentially binds to itself rather than Tysnd1-F. HeLa cells were co-transfected with a combination of plasmids encoding mutant ΔCv-WT or C-WT of HA-Tysnd1 and ΔCv-WT or C-WT of FLAG-Tysnd1 as indicated. The corresponding mock-transfected cells were analyzed as a control. Cells were subjected to immunoprecipitation using anti-FLAG IgG-conjugated agarose, and the immunoprecipitates were analyzed by SDS-PAGE and immunoblot using the antibodies indicated on the *left*. *Input*, 10% of the lysate used for immunoprecipitation (*IP*). *D*, Tysnd1 forms higher molecular mass complexes. Organelle fractions from HEK293 cells stably expressing FLAG-Tysnd1-WT and FLAG-Tysnd1-SA as well as control HEK293 cells were solubilized with 1% digitonin and then analyzed by blue native (*BN*) PAGE followed by immunoblot using anti-FLAG (*lanes 1–3*) and anti-Tysnd1 (*lanes 4–9*) antibodies. *Solid* and *open arrowheads* indicate the two major complexes of FLAG-Tysnd1. Molecular mass markers (*MK*) are on the *left*. The *asterisk* indicates a nonspecific band. *ADAPS*, alkyldihydroxyacetonephosphate synthase; *LDH*, lactate dehydrogenase; *exp.*, exposure.

We also assessed whether PsLon degrades the N- and C-fragments of Tysnd1 using CHO-K1 cells that co-expressed HA-PsLon and HA-PsLon-SA harboring a Ser^{743}-to-Ala substitution in the putative active site of the serine protease domain. Tysnd1-C and -N fragments derived from HA-Tysnd1-WT as well as ectopically expressed HA-Tysnd1-N were more readily detectable in CHO-K1 cells expressing HA-PsLon-SA or a control protein (EGFP-SKL) compared with HA-PsLon-expressing cells (Fig. 6*B*). Collectively, PsLon most likely degrades Tysnd1-N and -C fragments, the self-cleavage products of Tysnd1, thereby regulating the constituent composition of Tysnd1 hetero-oligomer complexes.

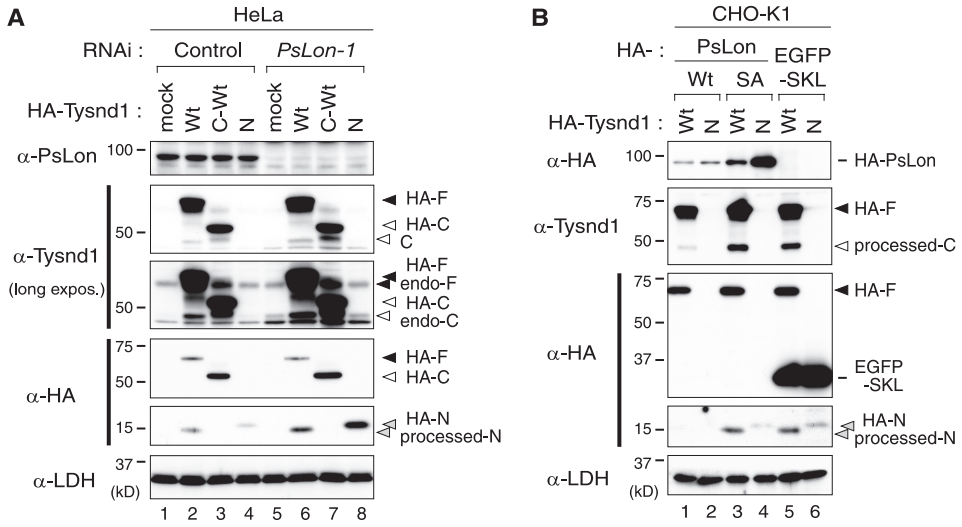

FIGURE 6. **PsLon preferentially degrades Tysnd1-C and Tysnd1-N.** *A*, knockdown of PsLon stabilizes the cleaved forms of Tysnd1, Tysnd1-C and Tysnd1-N. HeLa cells were transfected with a control siRNA (*lanes 1–3*) and *PsLon-1* siRNA (*lanes 4–6*). At 48 h post-transfection, cells were retransfected with the same siRNAs used in the initial transfection together with plasmids encoding HA-Tysnd1 variants. After 24 h, cells were lysed and analyzed by SDS-PAGE and immunoblot using the antibodies indicated on the *left*. The anti-Tysnd1 immunoblot is shown at normal (*upper panel*) and longer exposure (*expos.*) (*lower panel*). *HA-F*, HA-Tysnd1-WT; *HA-N*, HA-Tysnd1-N; *HA-C*, HA-Tysnd1-C; *endo-F*, endogenous Tysnd1; *endo-C*, endogenous Tysnd1-C; *processed-N*, Tysnd1-N derived from HA-Tysnd1-WT. *B*, overexpression of wild-type PsLon enhances the degradation of Tysnd1-N. CHO-K1 cells were transfected with plasmids encoding variants of HA-Tysnd1 and HA-PsLon variants along with FLAG-EGFP-SKL as indicated at the *top*. Cell lysates were verified by immunoblot as described for *A*. *processed-C* indicates Tysnd1-C derived from HA-Tysnd1-WT. Note that exogenously expressed HA-Tysnd1-N tagged with PTS1 (see Fig. 4*A*) migrated more slowly than the self-cleaved HA-Tysnd1-N fragment of full-length HA-Tysnd1-WT. *LDH*, lactate dehydrogenase.

Tysnd1 Is Involved in Regulation of Peroxisomal Fatty Acid β-Oxidation—Tysnd1 catalyzed the proteolytic processing of several enzymes involved in the peroxisomal fatty acid β-oxidation pathway (Figs. 3*A* and 4*C*), and the self-cleaved forms of Tysnd1 were degraded by PsLon (Fig. 6). These findings prompted us to investigate whether Tysnd1 and PsLon were linked to the regulation of peroxisomal fatty acid β-oxidation. Using a very long fatty acid, 1-^{14}C-labeled lignoceric acid (C24:0) as a substrate, peroxisomal fatty acid β-oxidation activity was assessed in HeLa cells that had been treated separately with *Tysnd1* and *PsLon* siRNAs as described under "Experimental Procedures." In cells treated with *Tysnd1-1* and *Tysnd1-2* siRNAs in which the level of PTS1 and PTS2 enzyme precursors was elevated depending on the knockdown efficiency (Fig. 3*A*), fatty acid β-oxidation activity was distinctly lowered to 68 and 42%, respectively, relative to cells treated with a control siRNA (Fig. 7). Under the same conditions as Tysnd1 knockdown, elimination of Pex5p by siRNA, which resulted in an import defect for all PTS1 and PTS2 proteins (Fig. 3*A*), resulted in an approximate 70% reduction of fatty acid β-oxidation activity compared with the control (Fig. 7). These results suggested that the knockdown of Tysnd1 lowers fatty acid β-oxidation by 80% relative to Pex5p elimination. Moreover, in two independent PsLon knockdown cell lines, fatty acid β-oxidation activity was decreased by about 30% compared with control cells. Taken together, these results indicated that Tysnd1 plays a pivotal role in the regulation of peroxisomal β-oxidation activity through proteolytic processing of β-oxidation enzymes. PsLon appears to regulate the expression levels of Tysnd1 through degradation of the self-processed forms of Tysnd1.

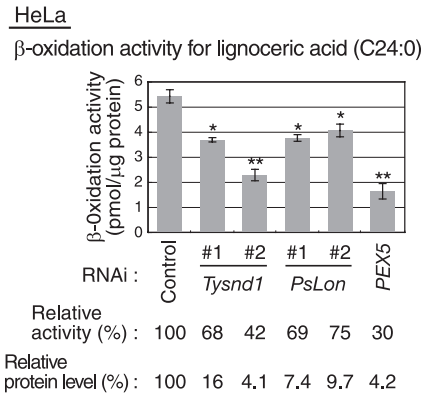

FIGURE 7. **Knockdown of Tysnd1 decreases β-oxidation of very long chain fatty acid lignoceric acid.** HeLa cells were transfected twice with various siRNAs as described for Fig. 3*A*. Cells were incubated at 37 °C for 2 h in serum-free medium containing 2 nmol of 1-^{14}C-labeled lignoceric acid (C24:0). β-Oxidation activity was determined by counting the radioactivity in the acid-soluble fractions and is expressed as pmol/h/μg of protein as described under "Experimental Procedures." *Error bars* represent the means ± S.E. of three independent experiments. *, $p < 0.05$; **, $p < 0.01$. β-Oxidation activity in siRNA-treated cells is also shown relative to that of control siRNA-treated cells, which was set as 100%.

DISCUSSION

Molecular mechanisms underlying peroxisome homeostasis, including protein turnover and enzyme regulation, remain largely unknown. The aim of the present work was to gain insight into such issues. Here, several lines of evidence are presented suggesting that two peroxisomal serine proteases, Tysnd1 and PsLon, coordinately maintain peroxisomal fatty acid β-oxidation through their protease activity.

Regulation of Proteolytic Processing Activity of Tysnd1—In both human and mouse, Tysnd1 is classified as an S1A subfamily trypsin-like serine protease along with Deg/HtrA proteases

(41). Although most Deg/HtrA proteases contain one to three PDZ domains in addition to a serine protease domain (42), Tysnd1 and its plant homologue *Arabidopsis* Deg15 are unique in that they are devoid of a PDZ domain (21, 43, 44). Mouse Tysnd1 was reported to function as a cysteine endopeptidase based on an inhibitor study in which only *N*-ethylmaleimide, but none of the serine protease inhibitors tested, inhibited Tysnd1 proteolytic activity (21). However, general serine protease inhibitors such as phenylmethylsulfonyl fluoride fail to inhibit a number of serine proteases, including *Escherichia coli* Deg protease P (45). Furthermore, the highly conserved catalytic triad His-Asp-Ser of Deg/HtrA proteases is present in Tysnd1 (His^{372}, Asp^{408}, and Ser^{481} in human Tysnd1) and Deg15 (44), and one of the catalytic triad residues, Ser^{481} of human Tysnd1, is essential for its proteolytic activity (Fig. 4), similar to Deg15 (44). Accordingly, Tysnd1 is most likely a serine protease.

Self-cleavage of authentic 60-kDa Tysnd1 gives rise to an N-terminal 15-kDa fragment and C-terminal 45-kDa fragment (21) (Figs. 3*A* and 4). However, the physiological role of this self-cleavage remained undefined. We showed here that full-length Tysnd1 is indeed an active protease and that self-cleavage of Tysnd1 down-regulates its protease activity (Fig. 4). The fact that the self-cleavage site of Tysnd1 is distantly located from its serine protease domain (Fig. 4*A*) suggests that self-cleavage-induced inactivation of Tysnd1 may be due to the loss of substrate recognition. How self-cleavage of Tysnd1 is regulated remains to be addressed in future work.

The substrate specificity of Tysnd1 appears to be somewhat complex. Mammalian Tysnd1 cleaves the presequence of PTS2 proteins and catalyzes the processing of PTS1 proteins involved in the peroxisomal β-oxidation of fatty acids (21) (Figs. 3*A* and 4). The cleavage site in the PTS2 precursor proteins TH and alkyldihydroxyacetonephosphate synthase is located just after a conserved cysteine residue (indicated with an asterisk) downstream of the PTS2 sequence AAPC*SAGF (6, 7) and TNEC*KARR (38), respectively. The PTS1-containing proteins AOx and SCPx on the other hand are processed at distinct sites, PQQV*AVWP (46) and AAPT*SSAG (37), respectively. In addition, Tysnd1 interacted with the PTS1-containing substrates AOx and SCPx but not with the PTS2 substrates TH and alkyldihydroxyacetonephosphate synthase in co-immunoprecipitation assays (Fig. 5, *A* and *B*). Tysnd1 also exhibited lower proteolytic activity *in vitro* against AOx compared with the TH precursor (21). Thus, it is plausible that there are distinct mechanisms that determine the substrate specificity of Tysnd1 perhaps involving oligomer formation with full-length and/or self-cleaved components (Fig. 5). It is noteworthy that glyoxysomal processing protease/Deg15, a Tysnd1 homologue in watermelon (*Citrullus vulgaris*), functions as a dimer in the proteolytic processing of PTS2 proteins as well as a monomer with general protease activity (43). Moreover, Deg/HtrA family proteases form trimeric, hexameric, and dodecameric complexes and exhibit dual functions in their different forms as exemplified by the chaperone and protease activities of Deg protease P (42). Thus, it is possible that dimeric, trimeric, and higher mass complexes of Tysnd1 (Fig. 5*D*) may possess distinct substrate specificities and protease activities. Tysnd1 isoforms were originally identified only in certain species of yeast, including *Yarrowia lipolytica* and *Candida albicans* (supplemental Table S2), but not in others such as *Saccharomyces cerevisiae* in which the PTS2 presequence is not cleaved in peroxisomes (8, 9). Tysnd1 isoforms and proteins specific for PTS2 targeting are absent from *Caenorhabditis elegans* (47), suggesting a functional link between the emergence of Tysnd1 and PTS2 proteins in multicellular organisms. Tysnd1 in higher eukaryotes such as plants and vertebrates (43) may have acquired additional protease specificities, including PTS2-cleaving activity, during evolution most likely in a manner highly correlated with the increasing complexity of peroxisome functions.

Significant accumulation of endogenous PTS1 and PTS2 protein precursors of the peroxisomal fatty acid β-oxidation pathway in Tysnd1-deficient HeLa cells (Fig. 3*A*) and CHO-K1 cells in which Tysnd1 was inactivated by a catalytic site mutation, S481A (Fig. 4), clearly demonstrated that the protease activity of Tysnd1 is essential for peroxisomal processing of PTS1 and PTS2 proteins. Furthermore, in Tysnd1 knockdown cells, there was a concomitant decrease in peroxisomal fatty acid β-oxidation activity (Fig. 7), strongly suggesting that the processing of PTS1 and PTS2 enzymes involved in β-oxidation is physiologically important for peroxisomal fatty acid β-oxidation. Nonspecific lipid transfer protein has been suggested to form complexes in peroxisomes with enzymes involved in fatty acid β-oxidation, including AOx, DBP, and TH, to efficiently catalyze the β-oxidation reaction (48). However, the physiological consequences of peroxisomal processing of PTS1 and PTS2 enzymes in terms of enzyme function remain less clear. For example, several reports have shown that the enzymatic activities of SCPx and DBP are not altered by processing (49–51). In the case of peroxisomal fatty acid β-oxidation, full-length AOx and the processed AOx fragments oligomerize to form heterodimers and homodimers of the full-length protein (40). Thus, Tysnd1-catalyzed processing of peroxisomal β-oxidation enzymes may give rise to the assembly of β-oxidation enzymes into larger enzyme complexes rather than modulate the catalytic activity of the respective enzymes. Meanwhile, we cannot exclude the possibility that Tysnd1 modulates an unidentified substrate protein that plays a key regulatory role in peroxisomal fatty acid β-oxidation.

Concerted Regulation of Peroxisomal Fatty Acid β-Oxidation by PsLon and Tysnd1—Three proteases have been identified in mammalian peroxisomes, including Tysnd1 (21), PsLon (23), and insulin-degrading enzyme (52). In an *in vitro* assay, insulin-degrading enzyme degraded the PTS2 presequence of rat TH (53) and oxidized lysozyme (54). In eukaryotes, mitochondrial Lon (mLon) is the major protease in the mitochondrial matrix involved in protein quality control, including degradation of misfolded or oxidized proteins (for reviews, see Refs. 22 and 55–57). Several mitochondrial substrates of mLon have been identified, including subunits of cytochrome *c* oxidase (58, 59), oxidized mitochondrial aconitase (60), steroidogenic acute regulatory protein StAR (61, 62), and mitochondrial transcription factor A (TFAM) (63).

To date, the functional role and substrates of PsLon in mammalian peroxisomes have been undefined. In the present work, we showed that the C- and N-terminal products of self-cleavage of full-length Tysnd1 are physiological substrates of PsLon (Figs. 3*A* and 6). Lon protease of *E. coli* recognizes clusters of hydrophobic

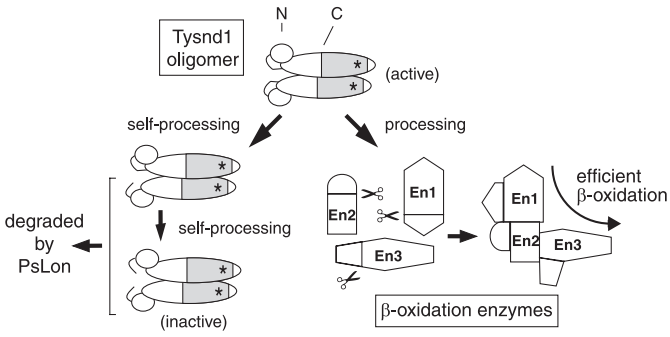

FIGURE 8. **Model for coordinated regulation of peroxisomal β-oxidation activity by Tysnd1 and PsLon.** Full-length Tysnd1 is active in the proteolytic processing of several enzymes involved in peroxisomal β-oxidation, including AOx and TH. Under normal conditions, a portion of Tysnd1 undergoes constitutive self-cleavage, which down-regulates its proteolytic processing activity. The self-cleaved and inactive forms of Tysnd1, Tysnd1-N and Tysnd1-C, are good substrates for PsLon and are rapidly degraded, whereby the peroxisomal β-oxidation pathway is regulated. Knockdown of Tysnd1 gives rise to the accumulation of premature or larger precursor forms of peroxisomal fatty acid β-oxidation enzymes and a decrease in total β-oxidation activity, suggesting that Tysnd1-catalyzed, constitutive processing of its substrate enzymes is required for maintaining the fatty acid β-oxidation pathway. See text for full details. *En*, enzyme. *Asterisks* indicates Ser^{481} in the protease domain of Tysnd1.

residues enriched in aromatic residues that are buried in the hydrophobic cores of native proteins but are exposed in misfolded proteins (64). Similarly, PsLon-catalyzed degradation of Tysnd1 is likely initiated by the self-cleavage of Tysnd1 and the resultant conformational changes of the Tysnd1 oligomer that give rise to exposed hydrophobic patches. Indeed, human Tysnd1 contains two aromatic residue-rich clusters, IFVPFL at positions 52–57 and FWAHFARLF at positions 143–151 in the N- and C-terminal regions, respectively. Likewise, PsLon probably also recognizes the N-terminal domain of DBP liberated by Tysnd1 processing as evidenced by the fact that this potential substrate of PsLon accumulated in *PsLon*-depleted HeLa cells (Fig. 3*A*). It is noteworthy that in cells separately expressing AOx and PsLon AOx was processed by PsLon with very low efficiency despite the fact that, in a stable HEK293 cell line ectopically expressing PsLon, PsLon interacted with AOx and several other peroxisomal β-oxidation enzymes in immunoprecipitation assays (65). In the current study, AOx processing in HeLa cells was not affected by treatment with *PsLon* siRNA (Fig. 3*A*). Moreover, AOx was not co-immunoprecipitated with PsLon from HEK/FL-PsLon-SA cells (data not shown), conditions under which AOx associated with FL-Tysnd1 (Fig. 5, *A* and *B*). These apparently inconsistent observations can nonetheless be reconciled; we propose that Tysnd1 mediates an indirect interaction between PsLon and AOx.

Physiological and functional roles of PsLon are suggested by the many reports of the requirement of mLon for multiple functions, including protein quality control in the mitochondria matrix (60, 63, 66, 67). Given that PsLon interacted with Tysnd1 (Fig. 5, *A*, *B*, and *C*) and PsLon knockdown significantly affected peroxisomal fatty acid β-oxidation activity (Fig. 7), we propose a working model in which Tysnd1 and PsLon regulate peroxisomal fatty acid β-oxidation in a concerted manner under normal physiological conditions (Fig. 8). Tysnd1 oligomers consisting of full-length Tysnd1 exhibit full proteolytic activity toward β-oxidation enzymes. As levels of the self-cleaved products increase, inactive oligomeric forms of Tysnd1 (Fig. 5*D*) also increase, and the protease activity of Tysnd1 decreases. PsLon appears to indirectly regulate peroxisomal fatty acid β-oxidation by degrading components of the protease-inactive Tysnd1 oligomer, thereby maintaining Tysnd1 turnover and activity and contributing to the regulation of the β-oxidation enzyme complex. Depletion of PsLon results in accumulation of the N- and C-terminal self-cleaved fragments of Tysnd1 in the oligomer but does not augment the processing of the DBP precursor or full-length Tysnd1 (Fig. 3*A*). Thus, self-cleavage of Tysnd1 in the active oligomer most likely inactivates its protease activity. Subsequently, the cleaved products are degraded by PsLon and removed from the Tysnd1 oligomer. Another possibility that is less likely but cannot be entirely ruled out is that Tysnd1 fragments in the Tysnd1 oligomer remain proteolytically active but are readily degraded by PsLon, resulting in protease inactivation. A physiological relationship between PsLon and Tysnd1 is also supported by a genetic interaction reported in *Arabidopsis thaliana* in which the growth defect in the plant PsLon homologue *lon2* mutant is enhanced by a defect in the Tysnd1 homologue DEG15 (68). Furthermore, mLon possesses chaperone-like activity in mitochondria that facilitates the assembly of protein complexes (58, 69). These lines of evidence support a regulatory role for PsLon in peroxisomal fatty acid β-oxidation.

All yeast species possess two Lon proteases, mLon and PsLon, with the exception of *S. cerevisiae* and *C. albicans*, which lack PsLon (70) (supplemental Table S2). This suggests a prerequisite for PsLon in lower eukaryotes. Although PsLon and Tysnd1 are both present in *Y. lipolytica* (43, 70) (supplemental Table S2), the functional association of PsLon and Tysnd1 such as that identified in *A. thaliana* (68) and in mammalian cells (this study) is more likely a consequence of co-evolution of the regulation of peroxisomal functions such as peroxisomal fatty acid β-oxidation. PsLon is also required for sustaining matrix protein import into peroxisomes in older cotyledon cells but not in younger ones as demonstrated in the *A. thaliana lon2* mutant (68). Peroxisomal import of matrix proteins was not affected by PsLon knockdown in HeLa cells (Fig. 3), although PsLon is believed to be involved in peroxisomal matrix protein import by virtue of the fact that peroxisomal localization of catalase is compromised by the overexpression of PsLon in HEK293 cells (65). Moreover, PsLon has been suggested to play a role in the degradation of various damaged proteins in peroxisomes based on analysis of a *pln* mutant of *Hansenula polymorpha* that is deficient in PsLon (70) and in the rapid clearance of fatty acid β-oxidation enzymes in rat hepatic cells after their release from di-(2-ethylhexyl)phthalate-induced peroxisome proliferation (71). Thus, PsLon may be involved in the degradation of several as yet unidentified substrates, including proteins that are involved in peroxisomal matrix protein import as well as those that function in stress responses and under normal conditions. In any event, prolonged depletion of PsLon as in PsLon knock-out mice would help uncover the functions and significance of PsLon in physiology and pathology in mammals.

Acknowledgments—We thank S. Okuno for technical assistance and M. Matsumoto for mass spectrometric analysis. We also thank M. Nishi for preparing figures and the other members of our laboratory for discussion.

REFERENCES

1. van den Bosch, H., Schutgens, R. B., Wanders, R. J., and Tager, J. M. (1992) *Annu. Rev. Biochem.* **61,** 157–197
2. Wanders, R. J., and Waterham, H. R. (2006) *Biochim. Biophys. Acta* **1763,** 1707–1720
3. Lazarow, P. B., and Fujiki, Y. (1985) *Annu. Rev. Cell Biol.* **1,** 489–530
4. Gould, S. J., Keller, G. A., Hosken, N., Wilkinson, J., and Subramani, S. (1989) *J. Cell Biol.* **108,** 1657–1664
5. Miura, S., Kasuya-Arai, I., Mori, H., Miyazawa, S., Osumi, T., Hashimoto, T., and Fujiki, Y. (1992) *J. Biol. Chem.* **267,** 14405–14411
6. Osumi, T., Tsukamoto, T., Hata, S., Yokota, S., Miura, S., Fujiki, Y., Hijikata, M., Miyazawa, S., and Hashimoto, T. (1991) *Biochem. Biophys. Res. Commun.* **181,** 947–954
7. Swinkels, B. W., Gould, S. J., Bodnar, A. G., Rachubinski, R. A., and Subramani, S. (1991) *EMBO J.* **10,** 3255–3262
8. Fujiki, Y., Okumoto, K., Kinoshita, N., and Ghaedi, K. (2006) *Biochim. Biophys. Acta* **1763,** 1374–1381
9. Platta, H. W., and Erdmann, R. (2007) *FEBS Lett.* **581,** 2811–2819
10. Brown, L. A., and Baker, A. (2003) *J. Cell. Mol. Med.* **7,** 388–400
11. Eckert, J. H., and Erdmann, R. (2003) *Rev. Physiol. Biochem. Pharmacol.* **147,** 75–121
12. Purdue, P. E., and Lazarow, P. B. (2001) *Annu. Rev. Cell Dev. Biol.* **17,** 701–752
13. Weller, S., Gould, S. J., and Valle, D. (2003) *Annu. Rev. Genomics Hum. Genet.* **4,** 165–211
14. Braverman, N., Dodt, G., Gould, S. J., and Valle, D. (1998) *Hum. Mol. Genet.* **7,** 1195–1205
15. Otera, H., Okumoto, K., Tateishi, K., Ikoma, Y., Matsuda, E., Nishimura, M., Tsukamoto, T., Osumi, T., Ohashi, K., Higuchi, O., and Fujiki, Y. (1998) *Mol. Cell Biol.* **18,** 388–399
16. Matsumura, T., Otera, H., and Fujiki, Y. (2000) *J. Biol. Chem.* **275,** 21715–21721
17. Mukai, S., and Fujiki, Y. (2006) *J. Biol. Chem.* **281,** 37311–37320
18. Wanders, R. J., and Waterham, H. R. (2006) *Annu. Rev. Biochem.* **75,** 295–332
19. Adamski, J., Normand, T., Leenders, F., Monté, D., Begue, A., Stéhelin, D., Jungblut, P. W., and de Launoit, Y. (1995) *Biochem. J.* **311,** 437–443
20. Leenders, F., Husen, B., Thole, H. H., and Adamski, J. (1994) *Mol. Cell. Endocrinol.* **104,** 127–131
21. Kurochkin, I. V., Mizuno, Y., Konagaya, A., Sakaki, Y., Schönbach, C., and Okazaki, Y. (2007) *EMBO J.* **26,** 835–845
22. Lee, I., and Suzuki, C. K. (2008) *Biochim. Biophys. Acta* **1784,** 727–735
23. Kikuchi, M., Hatano, N., Yokota, S., Shimozawa, N., Imanaka, T., and Taniguchi, H. (2004) *J. Biol. Chem.* **279,** 421–428
24. Okumoto, K., Abe, I., and Fujiki, Y. (2000) *J. Biol. Chem.* **275,** 25700–25710
25. Tsukamoto, T., Yokota, S., and Fujiki, Y. (1990) *J. Cell Biol.* **110,** 651–660
26. Otera, H., Nishimura, M., Setoguchi, K., Mori, T., and Fujiki, Y. (2001) *J. Biol. Chem.* **276,** 2858–2864
27. Honsho, M., Yagita, Y., Kinoshita, N., and Fujiki, Y. (2008) *Biochim. Biophys. Acta* **1783,** 1857–1865
28. Otera, H., Harano, T., Honsho, M., Ghaedi, K., Mukai, S., Tanaka, A., Kawai, A., Shimizu, N., and Fujiki, Y. (2000) *J. Biol. Chem.* **275,** 21703–21714
29. Shimizu, N., Itoh, R., Hirono, Y., Otera, H., Ghaedi, K., Tateishi, K., Tamura, S., Okumoto, K., Harano, T., Mukai, S., and Fujiki, Y. (1999) *J. Biol. Chem.* **274,** 12593–12604
30. Okumoto, K., Shimozawa, N., Kawai, A., Tamura, S., Tsukamoto, T., Osumi, T., Moser, H., Wanders, R. J., Suzuki, Y., Kondo, N., and Fujiki, Y. (1998) *Mol. Cell. Biol.* **18,** 4324–4336
31. Miyazawa, S., Osumi, T., Hashimoto, T., Ohno, K., Miura, S., and Fujiki, Y. (1989) *Mol. Cell. Biol.* **9,** 83–91
32. Tamura, S., Yasutake, S., Matsumoto, N., and Fujiki, Y. (2006) *J. Biol. Chem.* **281,** 27693–27704
33. Matsumoto, M., Hatakeyama, S., Oyamada, K., Oda, Y., Nishimura, T., and Nakayama, K. I. (2005) *Proteomics* **5,** 4145–4151
34. Honsho, M., Asaoku, S., and Fujiki, Y. (2010) *J. Biol. Chem.* **285,** 8537–8542,
35. Suzuki, Y., Shimozawa, N., Yajima, S., Yamaguchi, S., Orii, T., and Hashimoto, T. (1991) *Biochem. Pharmacol.* **41,** 453–456
36. Dodt, G., and Gould, S. J. (1996) *J. Cell Biol.* **135,** 1763–1774
37. Mori, T., Tsukamoto, T., Mori, H., Tashiro, Y., and Fujiki, Y. (1991) *Proc. Natl. Acad. Sci. U.S.A.* **88,** 4338–4342
38. de Vet, E. C., Zomer, A. W., Lahaut, G. J., and van den Bosch, H. (1997) *J. Biol. Chem.* **272,** 798–803
39. Chang, C. C., South, S., Warren, D., Jones, J., Moser, A. B., Moser, H. W., and Gould, S. J. (1999) *J. Cell Sci.* **112,** 1579–1590
40. Osumi, T., Hashimoto, T., and Ui, N. (1980) *J. Biochem.* **87,** 1735–1746
41. Rawlings, N. D., Tolle, D. P., and Barrett, A. J. (2004) *Nucleic Acids Res.* **32,** D160–D164
42. Clausen, T., Southan, C., and Ehrmann, M. (2002) *Mol. Cell* **10,** 443–455
43. Helm, M., Lück, C., Prestele, J., Hierl, G., Huesgen, P. F., Fröhlich, T., Arnold, G. J., Adamska, I., Görg, A., Lottspeich, F., and Gietl, C. (2007) *Proc. Natl. Acad. Sci. U.S.A.* **104,** 11501–11506
44. Schuhmann, H., Huesgen, P. F., Gietl, C., and Adamska, I. (2008) *Plant Physiol.* **148,** 1847–1856
45. Lipinska, B., Zylicz, M., and Georgopoulos, C. (1990) *J. Bacteriol.* **172,** 1791–1797
46. Miyazawa, S., Hayashi, H., Hijikata, M., Ishii, N., Furuta, S., Kagamiyama, H., Osumi, T., and Hashimoto, T. (1987) *J. Biol. Chem.* **262,** 8131–8137
47. Motley, A. M., Hettema, E. H., Ketting, R., Plasterk, R., and Tabak, H. F. (2000) *EMBO Rep.* **1,** 40–46
48. Wouters, F. S., Bastiaens, P. I., Wirtz, K. W., and Jovin, T. M. (1998) *EMBO J.* **17,** 7179–7189
49. Seedorf, U., Brysch, P., Engel, T., Schrage, K., and Assmann, G. (1994) *J. Biol. Chem.* **269,** 21277–21283
50. Antonenkov, V. D., Van Veldhoven, P. P., Waelkens, E., and Mannaerts, G. P. (1997) *J. Biol. Chem.* **272,** 26023–26031
51. van Grunsven, E. G., Mooijer, P. A., Aubourg, P., and Wanders, R. J. (1999) *Hum. Mol. Genet.* **8,** 1509–1516
52. Authier, F., Rachubinski, R. A., Posner, B. I., and Bergeron, J. J. (1994) *J. Biol. Chem.* **269,** 3010–3016
53. Authier, F., Bergeron, J. J., Ou, W. J., Rachubinski, R. A., Posner, B. I., and Walton, P. A. (1995) *Proc. Natl. Acad. Sci. U.S.A.* **92,** 3859–3863
54. Morita, M., Kurochkin, I. V., Motojima, K., Goto, S., Takano, T., Okamura, S., Sato, R., Yokota, S., and Imanaka, T. (2000) *Cell Struct. Funct.* **25,** 309–315
55. Friguet, B., Bulteau, A. L., and Petropoulos, I. (2008) *Biotechnol. J.* **3,** 757–764
56. Voos, W. (2009) *Res. Microbiol.* **160,** 718–725
57. Van Melderen, L., and Aertsen, A. (2009) *Res. Microbiol.* **160,** 645–651
58. *Hori, O., Ichinoda, F., Tamatani, T., Yamaguchi, A., Sato, N., Ozawa, K., Kitao, Y., Miyazaki, M., Harding, H. P., Ron, D., Tohyama, M., Stern, D. M., and Ogawa, S.* (2002) *J. Cell Biol.* **157,** 1151–1160
59. Fukuda, R., Zhang, H., Kim, J. W., Shimoda, L., Dang, C. V., and Semenza, G. L. (2007) *Cell* **129,** 111–122
60. Bota, D. A., and Davies, K. J. (2002) *Nat. Cell Biol.* **4,** 674–680
61. Ondrovicová, G., Liu, T., Singh, K., Tian, B., Li, H., Gakh, O., Perecko, D., Janata, J., Granot, Z., Orly, J., Kutejová, E., and Suzuki, C. K. (2005) *J. Biol. Chem.* **280,** 25103–25110
62. Granot, Z., Kobiler, O., Melamed-Book, N., Eimerl, S., Bahat, A., Lu, B., Braun, S., Maurizi, M. R., Suzuki, C. K., Oppenheim, A. B., and Orly, J. (2007) *Mol. Endocrinol.* **21,** 2164–2177
63. Matsushima, Y., Goto, Y., and Kaguni, L. S. (2010) *Proc. Natl. Acad. Sci. U.S.A.* **107,** 18410–18415
64. Gur, E., and Sauer, R. T. (2008) *Genes Dev.* **22,** 2267–2277
65. Omi, S., Nakata, R., Okamura-Ikeda, K., Konishi, H., and Taniguchi, H. (2008) *J. Biochem.* **143,** 649–660
66. Suzuki, C. K., Suda, K., Wang, N., and Schatz, G. (1994) *Science* **264,** 273–276
67. Wagner, I., Arlt, H., van Dyck, L., Langer, T., and Neupert, W. (1994) *EMBO J.* **13,** 5135–5145
68. Lingard, M. J., and Bartel, B. (2009) *Plant Physiol.* **151,** 1354–1365
69. Rep, M., van Dijl, J. M., Suda, K., Schatz, G., Grivell, L. A., and Suzuki, C. K. (1996) *Science* **274,** 103–106
70. Aksam, E. B., Koek, A., Kiel, J. A., Jourdan, S., Veenhuis, M., and van der Klei, I. J. (2007) *Autophagy* **3,** 96–105
71. Yokota, S., Haraguchi, C. M., and Oda, T. (2008) *Histochem. Cell Biol.* **129,** 73–83